

Contents lists available at ScienceDirect

# Journal of Biomechanics

journal homepage: [www.elsevier.com/locate/jbiomech](http://www.elsevier.com/locate/jbiomech)  
[www.JBiomech.com](http://www.JBiomech.com)



## A comprehensive, open-source dataset of lower limb biomechanics in multiple conditions of stairs, ramps, and level-ground ambulation and transitions

Jonathan Camargo <sup>a,b,\*</sup>, Aditya Ramanathan <sup>a</sup>, Will Flanagan <sup>a</sup>, Aaron Young <sup>a,b</sup>

<sup>a</sup> George W. Woodruff School of Mechanical Engineering, Georgia Institute of Technology, Atlanta, GA, USA

<sup>b</sup> Institute of Robotics and Intelligent Machines, Georgia Institute of Technology, Atlanta, GA, USA



### ARTICLE INFO

#### Article history:

Accepted 3 February 2021

#### Keywords:

Locomotion biomechanics  
Stairs  
Ramps  
Level-ground  
Treadmill  
Wearable sensors  
Open dataset

### ABSTRACT

We introduce a novel dataset containing 3-dimensional biomechanical and wearable sensor data from 22 able-bodied adults for multiple locomotion modes (level-ground/treadmill walking, stair ascent/descent, and ramp ascent/descent) and multiple terrain conditions of each mode (walking speed, stair height, and ramp inclination). In this paper, we present the data collection methods, explain the structure of the open dataset, and report the sensor data along with the kinematic and kinetic profiles of joint biomechanics as a function of the gait phase. This dataset offers a comprehensive source of locomotion information for the same set of subjects to motivate applications in locomotion recognition, developments in robotic assistive devices, and improvement of biomimetic controllers that better adapt to terrain conditions. With such a dataset, models for these applications can be either subject-dependent or subject-independent, allowing greater flexibility for researchers to advance the field.

© 2021 Elsevier Ltd. All rights reserved.

### 1. Introduction

The study of human movement using motion capture has been a fundamental aspect of biomechanics research ever since the pioneering photography work of Eadweard Muybridge and Etienne-Jules Marey in the late 1800s (Innocenti, 2017). Following its development, motion capture has become the standard for calculating joint kinematics (angular positions, velocities, accelerations) and kinetics (moments, powers) through skeletal modeling applications with external force data (Delp et al., 2007; Farris and Sawicki, 2012). Using this technology, many researchers have worked on characterizing human movement over various *locomotion modes* (level-ground/treadmill walking, stair ascent/descent, ramp ascent/descent) and *terrain conditions* (walking speed, ramp inclination, stair height) within each mode. While treadmill walking at different speeds is commonly studied (Lange et al., 1996; Ankarali et al., 2015), attention has been drawn towards other modes, such as ascending and descending stairs and ramps (Redfern and DiPasquale, 1997; Riener et al., 2002). These studies are crucial for determining human movement strategies in environments more prevalent to community ambulation. With the

advancement of data processing and machine learning techniques, the use of wearable sensing technology has also produced important contributions to the understanding of muscle coordination during locomotion (Sylos-Labini et al., 2014; Chvatal and Ting, 2012; Hug et al., 2019). By observing patterns in electromyography (EMG) signals during multiple activities, muscle activation has been related to anticipation of transitions (Peng et al., 2016), and individual, antagonistic, and cooperative muscular roles have been linked to specific motor tasks (Prilutsky et al., 1998; Ivanenko et al., 2006; Chvatal and Ting, 2013). As these patterns provide important information for the development of targeted rehabilitation methods and improvement of robotic control (Huang et al., 2011), comprehensive datasets that associate biomechanical characteristics with wearable sensor information would support the advances in rehabilitation and assistance programs. Furthermore, the inclusion of many locomotion modes and conditions better relate this information to daily living settings (Wolfinbarger and Shehab, 2000; Orendurff et al., 2005; Salbach et al., 2014; Orendurff, 2016).

Since research is often cumulative in nature, the impact of open datasets is immense. These resources greatly accelerate scientific advancement by encouraging new analyses, good data practices, and reproducibility (McKiernan et al., 2016). The most renowned open dataset within the biomechanics field comes from David A. Winter, whose 2-D walking dataset (Winter, 1983) is considered the standard for normative gait profiles. Although it has motivated

\* Corresponding author at: George W. Woodruff School of Mechanical Engineering, Georgia Institute of Technology, Atlanta, GA, USA.

E-mail address: [jon-cama@gatech.edu](mailto:jon-cama@gatech.edu) (J. Camargo).

many research ideas, the dataset only provides kinematic and kinetic data for level-ground and treadmill walking. As the field has outgrown this dataset and investigated locomotion over varying modes, perturbations, and data from wearable sensors, new and open resources to facilitate these studies are scarce. Some recent efforts have begun tackling this problem by generating open datasets for various locomotion activities, such as work from Moore et al. (2015), R.K. Fukuchi et al. (2017), Hu et al. (2018), C. A. Fukuchi et al. (2018), Schreiber and Moissenet (2019), and Lencioni et al. (2019). Moore's dataset and R.K. Fukuchi's dataset both contain kinematic data from able-bodied subjects on a treadmill at various speeds, with Moore including longitudinal perturbations in speed. Hu's dataset includes EMG, inertial measurement unit (IMU), and goniometer (GON) information for able-bodied subjects transitioning between locomotor activities consisting of level-ground, ramps, and stairs. C.A. Fukuchi's dataset presents kinematic data for level-ground walking and treadmill walking at different speeds from able-bodied subjects diverse in age. Schreiber's dataset is similar to C.A. Fukuchi's, containing kinematic data for level-ground walking at multiple speeds from able-bodied subjects diverse in age, with the notable inclusion of EMG. Lencioni's dataset contains kinematic and EMG data for level-ground walking at different speeds as well, along with the modes of toe-walking, heel-walking, stair ascent, and stair descent. In addition to these expansive datasets being critical for biomechanical analyses, they can also benefit the development of controllers for assistive devices (Tucker et al., 2015). For this application, however, one crucial limitation arises: in order to effectively cover the wide array of locomotion modes and terrain conditions that an assistive device may encounter in daily living, data would have to be combined from multiple sources and would thus contain many distinct sets of subjects. This restricts the development of controllers to subject-independent models, which typically perform worse than subject-dependent models (Young and Hargrove, 2016). To address this issue, researchers must have access to datasets containing a comprehensive range of modes and conditions for the same set of subjects.

This paper presents able-bodied human locomotion data from four different locomotion modes: level-ground walking, treadmill walking, ramps, and stairs. Each locomotion mode was evaluated at different terrain conditions: subject self-selected speeds for level-ground, belt speed for treadmill, ramp inclination, and stair height. Our contribution extends to the release of the experiment database, giving access to trial-specific information about the biomechanics and wearable signals. This dataset includes the joint-level kinematics, moments, and powers processed using inverse dynamics from the open-source biomechanics software OpenSim (Delp et al., 2007; Seth et al., 2018), along with data from multiple wearable sensors, namely EMG, GON, and IMU. A comprehensive dataset with motion capture and wearable sensor data over multiple modes/conditions will greatly assist data-driven analyses, such as the development of models for locomotion intent recognition. We expect this work to become a valuable source of biomechanics and wearable sensor data for different environments and conditions, as well as enabling the study of the effects of these conditions at the joint level. In addition to the dataset itself, we include a thorough description of the structure of the data with the hope that future works can expand this data bank to other populations, thus providing a more representative sample of human locomotion.

## 2. Methods

The experiment was conducted on 22 healthy adults (Table 1), age  $21 \pm 3.4$  yr, height  $1.70 \pm 0.07$  m, mass  $68.3 \pm 10.83$  kg. Subjects

were instrumented (Fig. 1) unilaterally on their right side with 11 EMG (Biometrics. Ltd. Newport, UK), 3 goniometers (Biometrics. Ltd. Newport, UK), 4 six-axis inertial measurement units (Yost, Ohio, USA), and bilaterally with 32 motion capture markers following the Helen Hayes Hospital marker set (Vicon. Ltd., Oxford, UK). Ground reaction forces were recorded using force plates (Bertec, Ohio, USA) located in the instrumented treadmill and level with the floor, ramp, and stairs (Fig. 2). All subjects provided informed consent, and the study was approved by the Georgia Institute of Technology IRB.

### 2.1. Data collection

Subjects performed trials in four different locomotion modes: treadmill walking, level-ground walking, ramp ascent/descent, and stair ascent/descent. Treadmill walking data were recorded for 28 speeds ranging from 0.5 to 1.85 m/s in 0.05 m/s increments. These speeds were interleaved over the course of 7 trials (4 speeds per trial) such that the subject started from rest, sped up to a slow speed, sped up again to a medium-fast speed, sped up once more to a fast speed, then slowed down to a medium-slow speed before stopping. Specifically, the speeds for the first treadmill trial were 0.5 m/s, 1.2 m/s, 1.55 m/s, and 0.85 m/s. All speeds were increased by 0.05 m/s for each subsequent trial (i.e. trial 2 was 0.55, 1.25, 1.6, 0.9 m/s). Each speed was held for 30 s between accelerations to capture steady-state walking. This stepped approach to collecting speeds allowed for larger amounts of acceleration data to be recorded.

Level-ground walking consisted of 5 clockwise circuits and 5 counterclockwise circuits at each of three different self-selected speeds: slow, normal, and fast, relative to the subject's preferred speed, for a total of 30 circuits per subject. As an analog to walking speed, pelvis linear velocity was calculated by averaging the total velocities of the four hip motion capture markers (ASISs and PSISs) over the steady-state walking sections to approximate the subject's walking speed. The average pelvis velocity over all subjects was found to be  $0.88 \pm 0.19$  m/s for the slow self-selected speed,  $1.17 \pm 0.21$  m/s for normal, and  $1.45 \pm 0.27$  m/s for fast.

Stair trials were executed at four different stair heights of a 6-step staircase within the range of ADA Accessibility Guidelines (Americans with Disabilities Act, 2010): 102 mm (4in), 127 mm (5in), 152 mm (6in), 178 mm (7in). For each stair height, subjects were instructed to complete a set of 5 trials starting with their instrumented leg and a set of 5 trials starting with their non-instrumented leg for a total of 40 stair trials.

Ramp trials were executed on a 5-meter long ramp at 6 inclination angles of  $5.2^\circ$ ,  $7.8^\circ$ ,  $9.2^\circ$ ,  $11^\circ$ ,  $12.4^\circ$ , and  $18^\circ$ . Similar to stairs, subjects completed a set of 5 trials for each starting leg at each incline for a total of 60 ramp trials. For both ramp and stair modes, subjects approached the mode from walking, transitioned onto the mode, ascended, transitioned off the mode, and came to a full stop at the top of the connected platform. Subjects then turned in place and descended the mode in a similar manner to complete one trial. A video of representative trials for each ambulation mode is provided in the [supplemental materials](#). The full instrumentation and data collection process for a single subject took 4–5 h, and all published data for a subject was recorded in a single experimental session. Subjects were allowed rest time between trials to prevent fatigue.

Raw EMG data were collected at a sampling frequency of 1000 Hz and digitally conditioned using a bandpass filter (cutoff frequency 20 Hz–400 Hz, Butterworth order 20). Lower limb muscles on the right side were targeted via palpation and SENIAM recommendations. The targeted muscles were: gluteus medius, right external oblique, semitendinosus, gracilis, biceps femoris, rectus femoris, vastus lateralis, vastus medialis, soleus, tibialis anterior,

**Table 1**

Physical characteristic information of each subject.

Subject ID	Age	Gender	Height (m)	Mass (kg)	Subject ID	Age	Gender	Height (m)	Mass (kg)
AB06	20	M	1.80	74.8	AB17	19	M	1.68	61.2
AB07	20	M	1.65	55.3	AB18	19	F	1.80	60.1
AB08	21	M	1.74	72.6	AB19	19	M	1.70	68.0
AB09	21	F	1.63	63.5	AB20	21	F	1.71	68.0
AB10	22	M	1.75	83.9	AB21	20	F	1.57	58.1
AB11	21	M	1.75	77.1	AB23	20	M	1.80	76.8
AB12	24	M	1.74	86.2	AB24	21	F	1.73	72.6
AB13	19	M	1.73	59.0	AB25	20	F	1.63	52.2
AB14	22	F	1.52	58.4	AB27	21	M	1.70	68.0
AB15	21	M	1.78	96.2	AB28	33	F	1.69	62.1
AB16	20	F	1.65	55.8	AB30	31	M	1.77	77.0

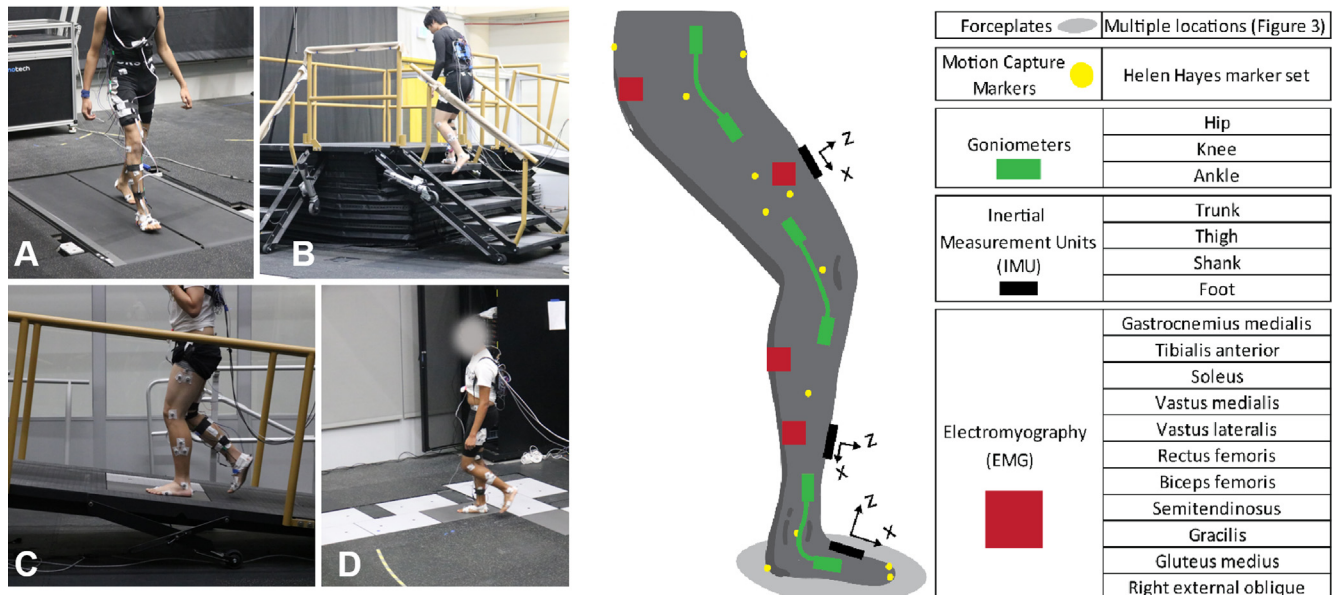


**Fig. 1.** (Left) Subjects performing ambulation modes. (A) treadmill walking, (B) stair-ascent, (C) ramp-ascent, (D) level-ground walking. (Right) Sensor placement. A combination of EMG, IMU, and electro-goniometers targeted major muscle groups, segments of the lower limb, and each of the three joints on the right side, while motion capture markers were placed bilaterally.

and gastrocnemius medialis. Prior to placement, EMG locations were shaved and cleaned with alcohol. IMU data were collected from the anterior surface of the torso, thigh, shank, and foot segments at a sampling frequency of 200 Hz and digitally processed with a lowpass filter (cutoff frequency 100 Hz, Butterworth order 6). For the thigh, shank, and foot, the IMU was placed  $\frac{3}{4}$  of the way down (distally) each segment of the right lower limb. The torso IMU was placed centrally between the sternum and navel. GON data were collected from the right-side hip, knee, and ankle joints at 1000 Hz and digitally conditioned with a lowpass filter (cutoff frequency 20 Hz, Butterworth order 4). Both sagittal and frontal angle data were recorded for the hip and ankle, while only sagittal angle data were collected for the knee.

Motion capture data collected at 200 Hz from both lower limbs were manually audited to verify labeling, and gaps were filled using an automated iterative gap-filling method (Camargo et al., 2020) before being processed with a lowpass filter (cutoff frequency 6 Hz, zero-lag Butterworth order 4). Ground reaction forces were measured at 1000 Hz and processed with a lowpass filter (cutoff frequency 15 Hz, zero-lag Butterworth order 10). Ground reaction forces were measured in all locomotion modes during certain representative steps, such as the transition steps to/from each mode and at least one steady-state step (Fig. 2).

The motion capture data and ground reaction force data were further analyzed with the inverse kinematics and inverse dynamics

tools from OpenSim (Seth et al., 2018) to determine the joint angles and moments in the sagittal, frontal, and transverse planes during the different locomotion tasks. To compute the joint powers for these planes, joint angles were numerically differentiated with MATLAB's *gradient* function and multiplied with the joint moments. Gait cycles without ground reaction force data were excluded from moment and power analyses. The reader may refer to the supplemental script *RUN\_OSIM.m* to replicate the processing of the inverse kinematics, inverse dynamics, and joint power.

## 2.2. Data access

The associated dataset is provided as [supplemental material](#) or can be accessed on <http://www.epic.gatech.edu/opensource-biomechanics-camargo-et-al/>. Data are stored as tables grouped by the nested directory structure of subject/date/mode/sensor (Fig. 3), allowing for easier access to trial information. Signals corresponding to the same trial can be aligned using a header column containing the time (seconds). This column is present in all the tables. The gait phase of each data point was also calculated using linear interpolation between heel strikes from 0% to 100% gait cycle. Heel strike was determined from the motion capture data as the point of zero linear velocity of the heel marker.

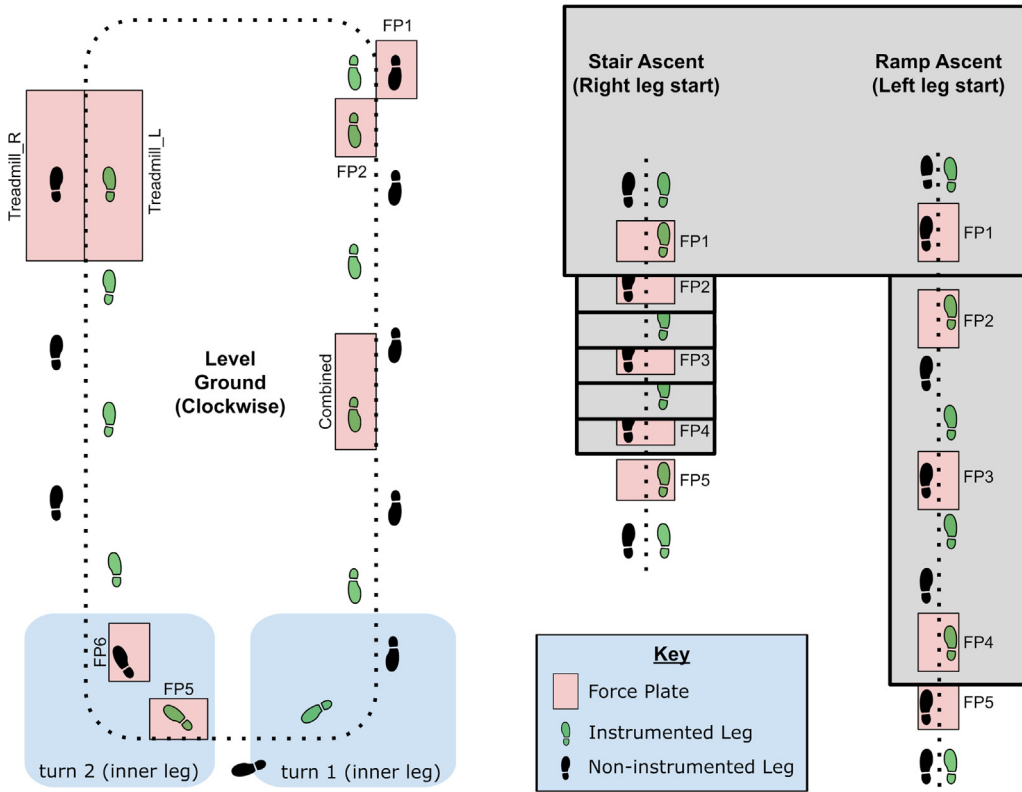


**Fig. 2.** Layout of the circuits in the experiment. Subjects performed trials over treadmill, level-ground, stair ascent and descent, ramp ascent, and descent modes. Force plates are placed in-ground for representative steps of the instrumented (right) leg and the non-instrumented (left) leg.

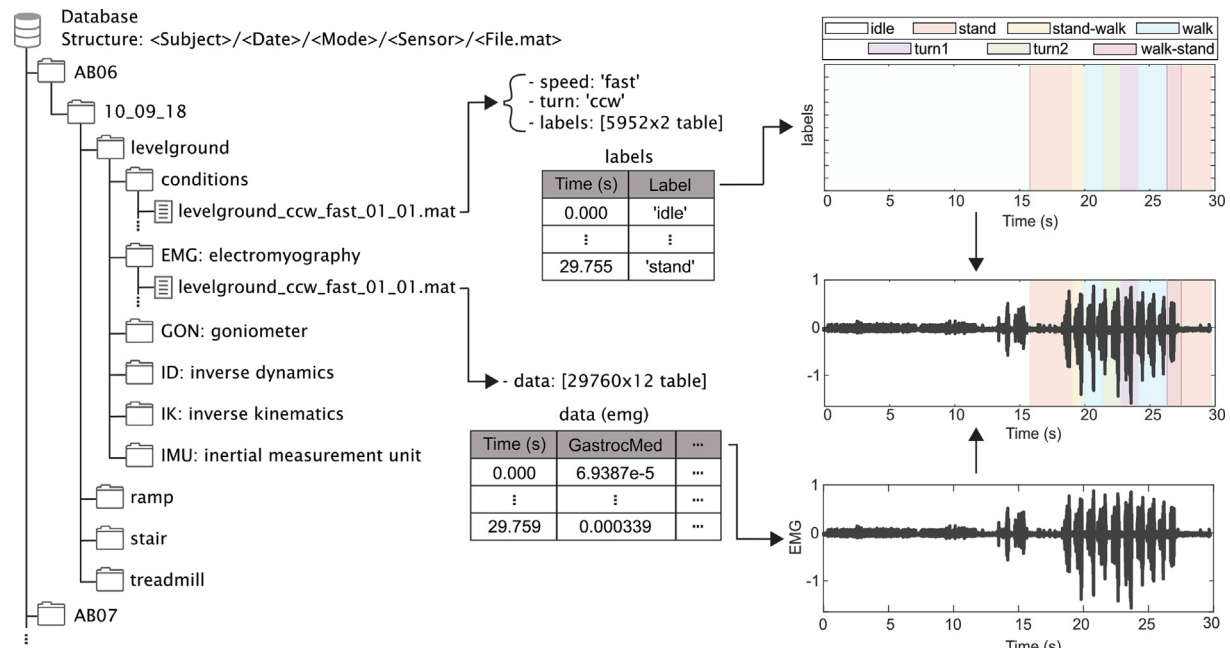


**Fig. 3.** Data structure for the open-source biomechanics database. The information is stored in nested folders, grouped by subject, date, locomotion mode, and sensor. Tables contain the information of each channel of a sensor type and the time index in the first column. The database is provided as supplemental material.

### 2.3. Example of use

Accompanying the dataset, we provide sample scripts to demonstrate its usage. The script *PLOT\_TRIAL.m* introduces the dataset structure and plots the raw data of an individual trial. *STRIDES.m* shows how to segment the data into strides based on

the gait cycle calculated from heel strikes. Finally, the script *PLOT\_STRIDES.m* uses the results from *STRIDES.m* to generate the gait profiles that are reported in the results section.

It is important to note that within the *STRIDES.m* script, we perform additional processing on the kinetics and the raw EMG. For the kinetics, the joint moments and powers are normalized by

the subject mass. For EMG, the signal envelope was obtained by rectifying and lowpass filtering (6 Hz cutoff) the raw data. The envelope amplitude was then normalized within each subject to better illustrate the common patterns of muscle activation during these locomotion activities across subjects. This is required due to the numerous factors that influence the signal, such as skin condition, electrode placement, and anatomical differences between subjects. Many normalization methods for EMG exist in the literature. However, in this case, EMG was normalized with respect to the average amplitude of the rectified signal for each subject over treadmill walking steps at 1.35 m/s. This technique was chosen as it reduces inter-subject variability (Burden, 2010), and the reference speed was chosen near the normal level-ground walking speed of able-bodied men and women of this age group (Bohannon and Andrews, 2011).

Using the results from these demonstrational scripts, we report the kinematics and kinetic profiles for each transition and steady-state ambulation mode. In addition, we investigated whether changes in the sagittal-plane biomechanics and wearable sensor data could be explained by a linear relationship with the terrain

condition within each locomotion mode. At each point in the gait cycle, a linear regression model was fit to the data to find the relationship between the biomechanics/wearable sensor variable and the terrain condition. To determine the statistical significance, the variance explained by the linear model was computed and tested against the null hypothesis of a model with zero coefficient ( $\alpha = 0.01$ ). This analysis resulted in the locations in the gait cycle where there is a significant linear relationship between the biomechanics/wearable sensor variable and the terrain condition.

### 3. Results

Kinematic and kinetic profiles for each locomotion mode are presented, reporting the 22 subject average profile for each condition within the mode. For treadmill walking, Fig. 4 shows the biomechanics profiles of the hip, knee, and ankle joints over the gait cycle. These profiles consist of the joint angle (deg), joint moment (Nm/kg), and joint power (W/kg). Moment and power are normalized to subject mass. The direction of joint motion is denoted by arrows marking flexion/extension; this convention is

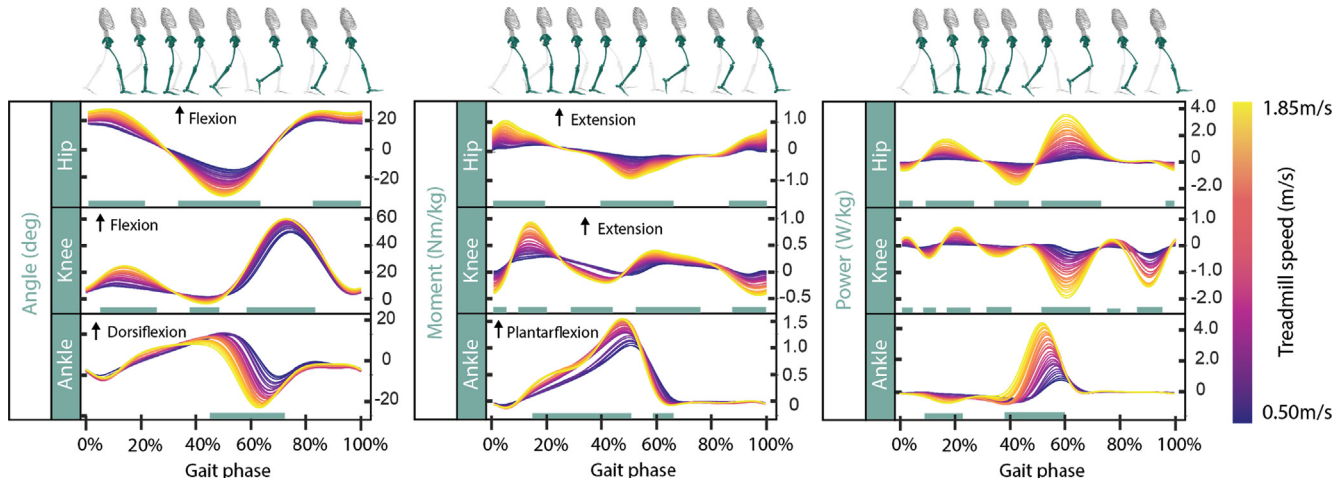


**Fig. 4.** Treadmill walking at different speeds ranging from 0.5 to 1.85 (m/s). Kinematics (left), moment normalized by subject weight (center), and power normalized by subject weight (right). The biomechanics profiles are normalized by the gait cycle defined from heel strike to heel strike of the right leg. At the top of each pane, the skeletal system shows the approximate body posture for that gait location. Horizontal bars denote a significant linear relationship between the biomechanics and the walking speed ( $p < 0.01$ ).

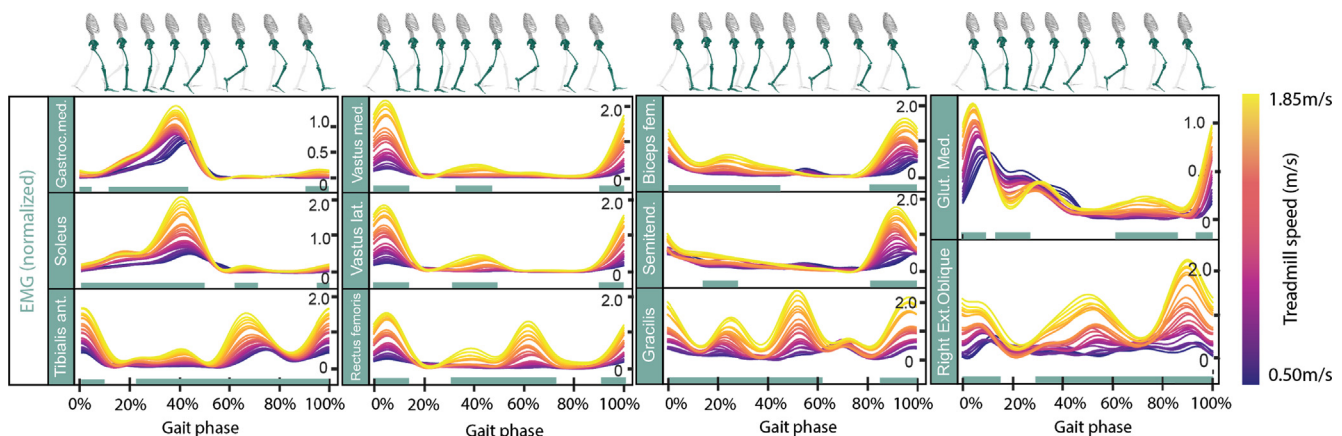


**Fig. 5.** Normalized EMG profiles for treadmill walking. EMG is rectified and normalized in magnitude to the average EMG walking at 1.35 m/s. The plot shows the profiles for the 11 different muscles captured at different conditions of speed ranging from 0.5 to 1.85 (m/s). The profiles are normalized to the gait cycle defined from heel strike to heel strike of the right leg. At the top of each pane, the skeletal system shows the approximate body posture for that gait location. Horizontal bars above the x-axis denote sections of gait cycle with a significant linear relationship between the amplitude of EMG and walking speed ( $p < 0.01$ ).

used consistently for all ambulation modes. The gait cycle profiles are color-coded based on the condition (treadmill speed, ramp inclination, stair height). Regions where the biomechanical variable had a significant ( $p < 0.01$ ) linear relationship with the terrain condition are marked with green horizontal bars on the x-axis. These patterns were observed at every joint, seen as a general increase in the ranges of motion, moments, and powers. A specific example of this is found during treadmill walking, where an increased walking speed corresponded to a significant increase in hip extension and ankle plantarflexion during push-off ( $p < 0.01$ ).

The same process can be applied to signals from wearable sensors. As an example of this, Fig. 5 shows the EMG envelope profiles over the gait cycle, normalized by the average amplitude for each subject walking at 1.35 m/s on the treadmill. The amplitude of the EMG envelope consistently increases as the walking speed increases, especially during periods of peak muscle activation.

The green horizontal bars in the x-axis highlight the sections of the gait cycle with statistical significance for the linear regression model. Kinematics and kinetic profiles for the other locomotion modes are presented in Figs. 6–8 and their corresponding EMG profiles can be found in the [supplemental materials](#), along with some example profiles of IMU (x-axis acceleration, y-axis angular velocity) and GON (sagittal plane) signals.

#### 4. Discussion

Recent efforts have begun to address the need for published biomechanics data beyond Winter's seminal dataset. These new datasets contain data from various locomotion modes or multiple terrain conditions of the same mode. However, none of these datasets contain both. This results in multiple datasets having to be combined to fully encompass the wide range of environments of

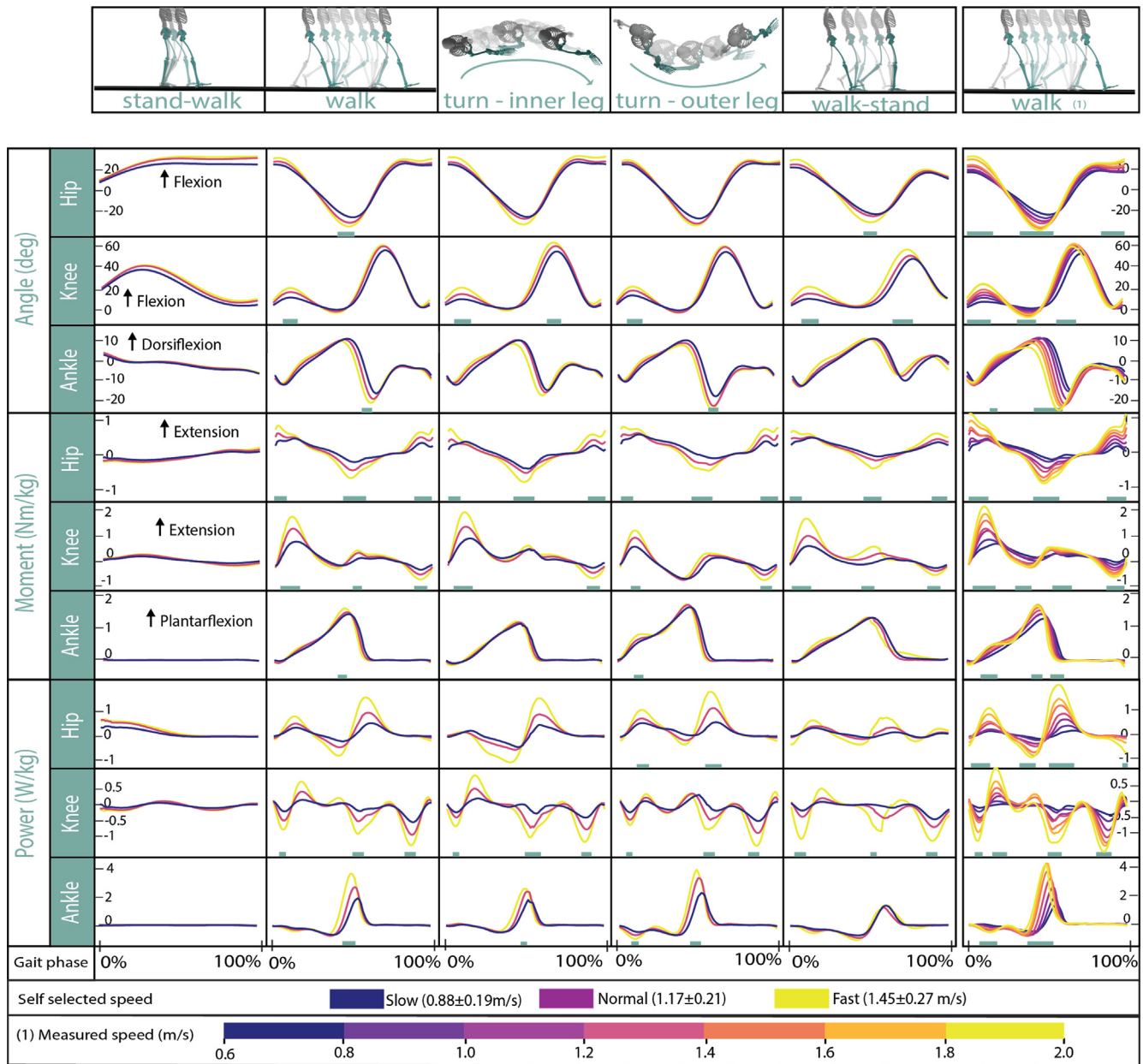


**Fig. 6.** Level-ground walking at different conditions of subject speed. Horizontal bars denote sections of the gait cycle where there is significant linear relation between biomechanics and walking speed ( $p < 0.01$ ). All modes except for the second walking segment split speeds based on the subject's self-selection, while the second walking segment bins the data based on the magnitude of the pelvis linear velocity <sup>(1)</sup> to better compare the data to treadmill walking.

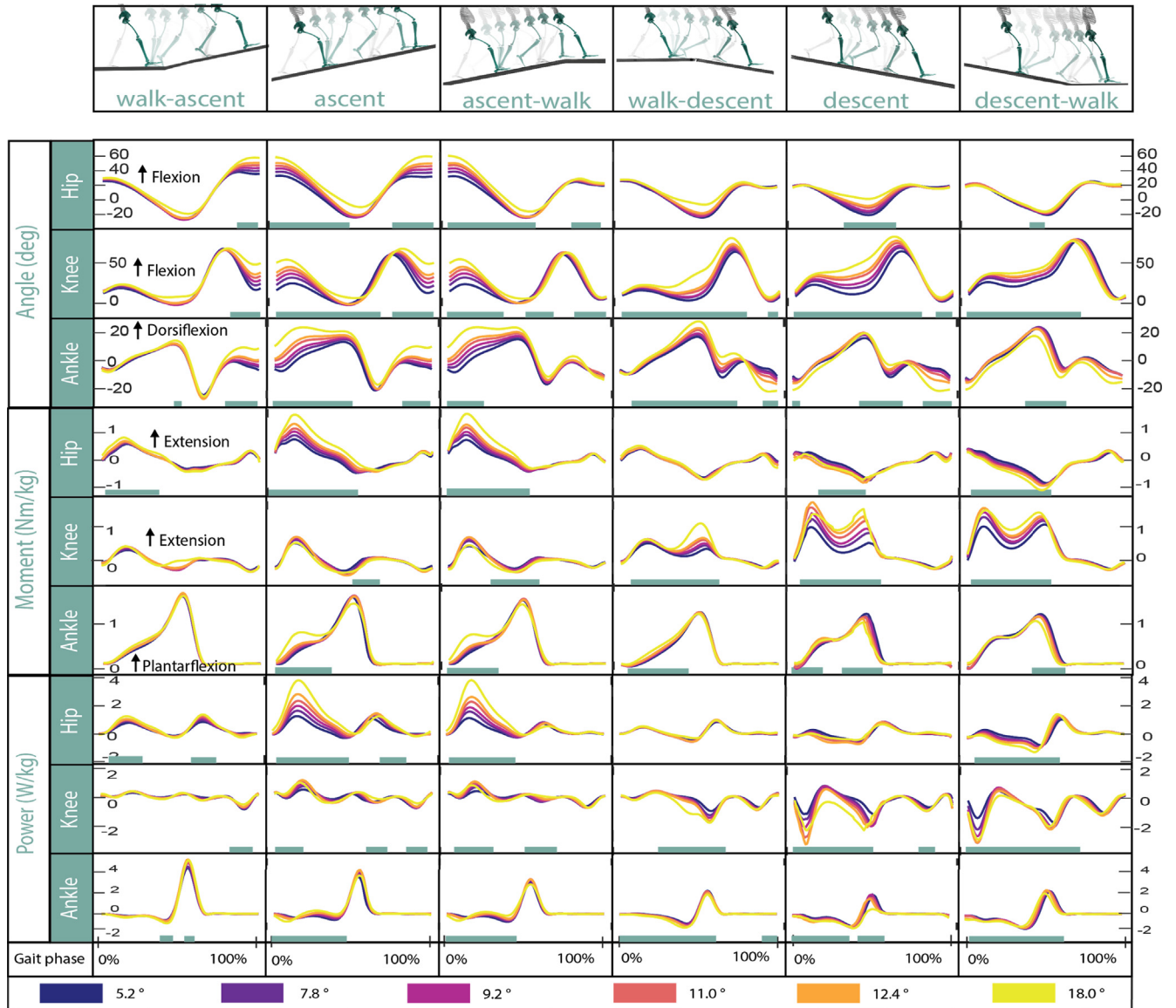


**Fig. 7.** Ramp ascent/descent at different conditions of ramp inclination ranging from 5.2° to 18.0°. Horizontal bars denote sections of the gait cycle where there is a significant linear relationship between the biomechanics and the ramp incline ( $p < 0.01$ ).

daily living. While this can be acceptable for biomechanical analysis, it severely limits the dataset's utility for applications such as locomotion recognition and the development of controllers for assistive devices by restricting them to subject-independent models. This paper aims to address this limitation and accelerate scientific progress through the creation of an open-source dataset for able-bodied locomotion over multiple locomotion modes and terrain conditions for the same set of subjects.

Open-source datasets facilitate the development of new methods and provide a benchmark for establishing comparisons (McKiernan et al., 2016). Some studies have released datasets of biomechanics, but to our best knowledge, the only references that include both biomechanics and wearable sensors are from Hu et al. (2018), Schreiber, and Moissenet (2019), and Lencioni et al. (2019). Hu's dataset contains GON, IMU, and EMG data for a single configuration of stairs and ramps. The other two datasets contain kinematics from motion capture and force plates along with EMG for level-ground walking at different speeds. Lencioni's dataset also includes kinetics data and the additional modes of toe-walking, heel-walking, and stair ascent/descent. Our contribution expands

the benefit of providing wearable sensor data related to kinematics by generating the resulting inverse dynamics and joint power evaluation for all modes and conditions, and it extends the terrain context by evaluating transitions and multiple conditions of walking speed, ramp inclination, and stair height. This comprehensive data of locomotion for the same set of subjects has never been provided to the biomechanics community and has important implications for high interest problems, such as the recognition of locomotion intent. This is critical for assistive devices (Long et al., 2018) and active prostheses (Young et al., 2014) to enable functionality beyond clinical settings. Such systems propose training AI models, which require information beyond the biomechanics, such as signals from wearable sensors like EMG, IMU, and goniometers. All of these signals are provided by our dataset. Capturing different terrain conditions within the same locomotion mode is also important to elucidate the patterns of joint-level changes within different contexts of ambulation (Orendurff, 2016). These patterns can be found in the dataset by investigating the effects of the terrain condition (walking speed, ramp inclination, and stair height) on the biomechanics profiles in terms of joint kinematics, moments,

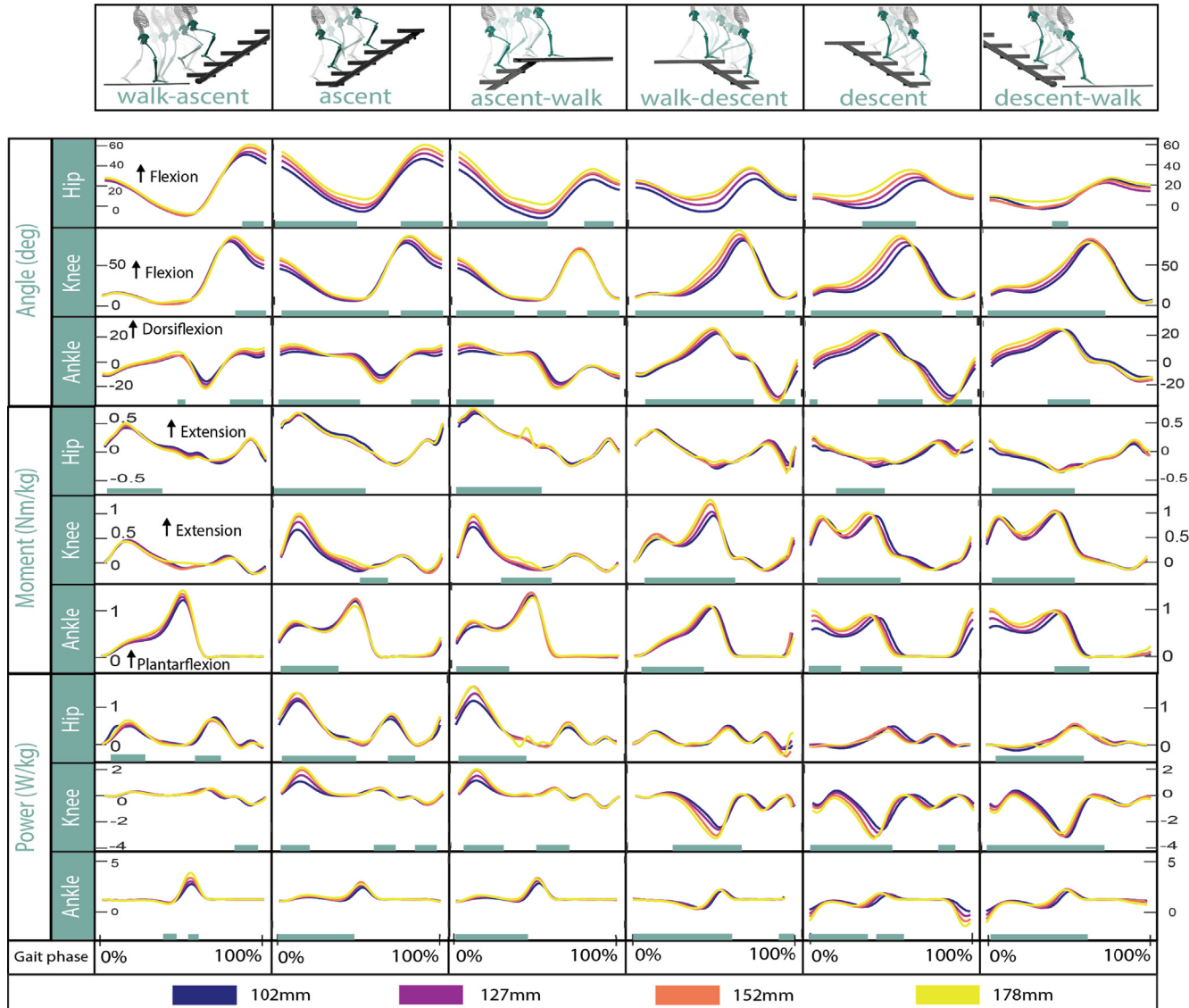


**Fig. 8.** Stair ascent/descent at different conditions of stair height ranging from 102 mm to 178 mm. Horizontal bars denote sections of the gait cycle where there is a significant linear relationship between the biomechanics and the stair height ( $p < 0.01$ ).

and powers along with the wearable sensor amplitudes. While this study only explored linear relationships between variables and the terrain condition, future work should examine possible higher order relationships.

Although this study contains comprehensive data for many locomotion modes and terrain conditions, several limitations must be noted. First, this study has a smaller sample size compared to some recent datasets (Schreiber and Moissenet, 2019; C.A. Fukuchi et al., 2018; Lencioni et al., 2019). However, our sample of 22 subjects is on par with other references that evaluated fewer conditions per subject (Moore et al., 2015; Hu et al., 2018; R.K. Fukuchi et al., 2017). Second, data were collected from a narrow demographic of young, healthy adults with no locomotive disabilities. While this population can serve as an exemplar for human locomotion, it does not intend to cover all variations that may result from age or disability. Third, although motion capture was collected bilaterally, wearable sensors were only placed on the right side. This unilateral instrumentation was appropriate for able-bodied locomotion; however, the assumption of gait

symmetry may be invalid for clinical populations. Finally, this dataset does not contain biomechanical data for the upper body or from clinical tests such as sit-to-stand. To better represent whole-body contributions to locomotion and address patient populations, we encourage the scientific community to follow the guidelines established in this paper and extend the data bank of locomotion biomechanics to other populations, testing procedures, and instrumentation arrangements.

## 5. Conclusions

Open datasets such as those provided by Winter have had a tremendous impact on scientific research into human locomotion. We aim to enhance these efforts by providing 3-dimensional biomechanical and wearable sensor data for able-bodied adults during multiple locomotion modes and terrain conditions. This dataset offers valuable information for future work in biomechanics, robotic assistive devices, and pattern recognition for community ambulation.

## Reference Data

Data available in data repository at Part 1/3: <http://dx.doi.org/10.17632/fcgm3chfff.1>; Part 2/3: <http://dx.doi.org/10.17632/k9kvm5tn3f.1>; Part 3/3: <http://dx.doi.org/10.17632/jj3r5f9pnf.1>.

## Declaration of Competing Interest

The authors declare that they have no known competing financial interests or personal relationships that could have appeared to influence the work reported in this paper.

## Acknowledgments

The authors would like to thank the members of the Sensor Fusion and Biomechanics team at the Exoskeleton and Prosthetic Intelligent Control lab at Georgia Institute of Technology.

## Appendix A. Supplementary material

Supplementary data to this article can be found online at <https://doi.org/10.1016/j.jbiomech.2021.110320>.

## References

- Ankarali, M.M. et al., 2015. Walking dynamics are symmetric (enough). *J. R. Soc. Interface* 12 (108), 20150209.
- Bohannon, R.W., Andrews, A.W., 2011. Normal walking speed: a descriptive meta-analysis. *Physiotherapy* 97, 182–189.
- Burden, A.M., 2010. How should we normalize electromyograms obtained from healthy participants? What we have learned from over 25 years of research. *J. Electromyogr. Kinesiol.* 20 (6), 1023–1035.
- Camargo, J., Ramanathan, A., Csomay-Shanklin, N., Young, A., 2020. Automated Gap-Filling for Marker-Based Biomechanical Motion Capture Data. *Computer Methods in Biomechanics and Biomedical Engineering*, s.l..
- Americans with Disabilities Act, 2010. CHAPTER 5: General site and building elements, in: Americans with Disabilities Act Standards. s.l.:s.n., p. 128.
- Chvatal, S.A., Ting, L.H., 2012. Voluntary and Reactive Recruitment of Locomotor Muscle Synergies during Perturbed Walking. *32(35)*, 12237–12250.
- Chvatal, S.A., Ting, L.H., 2013. Common muscle synergies for balance and walking. *Front. Comput. Neurosci.* 7, 1–14.
- Delp, S.L. et al., 2007. OpenSim: open-source software to create and analyze dynamic simulations of movement. *IEEE Trans. Biomed. Eng.* 54 (11), 1940–1950.
- Farris, D.J., Sawicki, G.S., 2012. The mechanics and energetics of human walking and running: a joint level perspective. *J. R. Soc. Interface* 9 (66), 110–118.
- Fukuchi, C.A., Fukuchi, R.K., Duarte, M., 2018. A public dataset of overground and treadmill walking kinematics and kinetics in healthy individuals. *PeerJ* 6, e4640.
- Fukuchi, R.K., Fukuchi, C.A., Duarte, M., 2017. A public dataset of running biomechanics and the effects of running speed on lower extremity kinematics and kinetics. *PeerJ* 5, e3298.
- Huang, H. et al., 2011. Continuous locomotion-mode identification for prosthetic legs based on neuromuscular-mechanical fusion. *IEEE Trans. Biomed. Eng.* 58 (10), 2867–2875.
- Hu, B., Rouse, E., Hargrove, L., 2018. Benchmark datasets for bilateral lower-limb neuromechanical signals from wearable sensors during unassisted locomotion in able-bodied individuals. *Front. Robot. AI* 5, 14.
- Hug, F. et al., 2019. Individuals have unique muscle activation signatures as revealed during gait and pedaling. *J. Appl. Physiol.* 127, 1165–1174.
- Innocenti, Bernardo, 2017. Biomechanics: a fundamental tool with a long history (and even longer future!). *Muscles Ligaments Tendons J.* 7, 491–492.
- Ivanenko, Y.P., Poppele, R.E., Lacquaniti, F., 2006. Motor control programs and walking. *Neuroscientist* 12 (4), 339–348.
- Lange, G.W. et al., 1996. Electromyographic and kinematic analysis of graded treadmill walking and the implications for knee rehabilitation. *J. Orthop. Sports Phys. Ther.* 23 (5), 294–301.
- Lencioni, T. et al., 2019. Human kinematic, kinetic and EMG data during different walking and stair ascending and descending tasks. *Sci Data* 6, 309.
- Long, Y., Du, Z.-J., Wang, W.-D., Dong, W., 2018. Human motion intent learning based motion assistance control for a wearable exoskeleton. *Robot. Comput. Integrated Manuf.* 49, 317–327.
- McKiernan, E.C. et al., 2016. How open science helps researchers succeed. *eLife* 5, e16800.
- Moore, J.K., Hnat, S.K., van den Bogert, A.J., 2015. An elaborate data set on human gait and the effect of mechanical perturbations. *PeerJ* 3, e918.
- Orendurff, M.S., 2016. Gait during real-world challenges: gait initiation, gait termination, acceleration, deceleration, turning, slopes, and stairs. In: Müller, B., Wolf, S. (Eds.), *Handbook of Human Motion*. Springer, s.l..
- Orendurff, M.S., Segal, A.D., Aiona, M.D., Dorociak, R.D., 2005. Triceps surae force, length and velocity during walking. *Gait & Posture* 21 (2), 157–163.
- Peng, J., Fey, N.P., Kuiken, T.A., Hargrove, L.J., 2016. Anticipatory kinematics and muscle activity preceding transitions from level-ground walking to stair ascent and descent. *J. Biomech.* 48 (4), 528–536.
- Prilutsky, B.I., Gregor, R.J., Ryan, M.M., 1998. Coordination of two-joint rectus femoris and hamstrings during the swing phase of human walking and running. *Exp. Brain Res.* 120 (4), 479–486.
- Redfern, M.S., DiPasquale, J., 1997. Biomechanics of descending ramps. *Gait and Posture* 6 (2), 119–125.
- Riener, R., Rabuffetti, M., Frigo, C., 2002. Stair ascent and descent at different inclinations. *Gait and Posture* 15, 32–44.
- Salbach, N.M. et al., 2014. Speed and distance requirements for community ambulation: a systematic review. *Arch. Phys. Med. Rehabil.* 95 (1), 117–128.
- Schreiber, C., Moissenet, F., 2019. A multimodal dataset of human gait at different walking speeds established on injury-free adult participants. *Sci. Data* 6 (1), 111.
- Seth, A. et al., 2018. OpenSim: Simulating musculoskeletal dynamics and neuromuscular control to study human and animal movement. *Public Library Sci.* 14, 1–20.
- Silos-Labini, F. et al., 2014. EMG patterns during assisted walking in the exoskeleton. *Front. Hum. Neurosci.* 8 (423), 1–12.
- Tucker, M.R. et al., 2015. Control strategies for active lower extremity prosthetics and orthotics: a review. *J. NeuroEng. Rehabil.* 12 (1).
- Winter, D.A., 1983. Biomechanical Motor Patterns in Normal Walking. *J. Mot. Behav.* 15, 302–330.
- Wolfsonbarger, K.G., Shehab, R.L., 2000. A survey of ramp and stair use among older adults. *Proc. Human Factors Ergon. Soc. Annual Meeting* 44 (24), 4–76–4–79.
- Young, A., Simon, A., Fey, N., Hargrove, L., 2014. Intent recognition in a powered lower limb prosthesis using time history information. *Ann. Biomed. Eng.* 42 (3), 631–641.
- Young, A., Hargrove, L., 2016. A classification method for user-independent intent recognition for transfemoral amputees using powered lower limb prostheses. *Trans. Neural Syst. Rehabilit. Eng.* 24 (2), 217–225.